Creating and verifying a quantum superposition in a micro-optomechanical system

Kleckner, D.; Pikovski, I.; Jeffrey, E.R.; Ament, L.J.P.; Eliel, E.R.; Brink, J. van den; Bouwmeester, D.

Creating and verifying a quantum superposition in a micro-optomechanical system

2008 New J. Phys. 10 095020

(http://iopscience.iop.org/1367-2630/10/9/095020)

New Journal of Physics
The open-access journal for physics

Creating and verifying a quantum superposition in a micro-optomechanical system

Dustin Kleckner[1,6,7], Igor Pikovski[2,3,6,7], Evan Jeffrey[2], Luuk Ament[4], Eric Eliel[2], Jeroen van den Brink[4,5] and Dirk Bouwmeester[1,2]

[1] Physics Department, University of California, Santa Barbara, CA 93106-9530, USA
[2] Huygens Laboratory, Universiteit Leiden, PO Box 9504, 2300 RA Leiden, The Netherlands
[3] Fachbereich Physik, Freie Universität Berlin, Arnimalle 14, 14195 Berlin, Germany
[4] Institute-Lorentz for Theoretical Physics, Universiteit Leiden, PO Box 9506, NL-2300 RA Leiden, The Netherlands
[5] Institute for Molecules and Materials, Radboud Universiteit Nijmegen, PO Box 9010, NL-6500 GL Nijmegen, The Netherlands
E-mail: dkleckner@physics.ucsb.edu and pikovski@molphys.leidenuniv.nl

New Journal of Physics **10** (2008) 095020 (18pp)
Received 5 May 2008
Published 30 September 2008
Online at http://www.njp.org/
doi:10.1088/1367-2630/10/9/095020

Abstract. Micro-optomechanical systems are central to a number of recent proposals for realizing quantum mechanical effects in relatively massive systems. Here, we focus on a particular class of experiments which aim to demonstrate massive quantum superpositions, although the obtained results should be generalizable to similar experiments. We analyze in detail the effects of finite temperature on the interpretation of the experiment, and obtain a lower bound on the degree of non-classicality of the cantilever. Although it is possible to measure the quantum decoherence time when starting from finite temperature, an unambiguous demonstration of a quantum superposition requires the mechanical resonator to be in or near the ground state. This can be achieved by optical cooling of the fundamental mode, which also provides a method to measure the mean phonon number in that mode. We also calculate the rate of environmentally induced decoherence and estimate the timescale for

[6] These authors contributed equally to this work.
[7] Authors to whom any correspondence should be addressed.

gravitational collapse mechanisms as proposed by Penrose and Diosi. In view of recent experimental advances, practical considerations for the realization of the described experiment are discussed.

Contents

1. Introduction

Micro-optomechanical systems have recently attracted significant interest as a potential architecture for observing quantum mechanical effects on scales many orders of magnitude more massive than previous experiments. Proposals include entangling states of mechanical resonators to each other [1]–[3] or cavity fields [4, 5], the creation of entangled photon pairs [6], ground state optical feedback cooling of the fundamental vibrational mode [7]–[11], observation of discrete quantum jumps [12], quantum state transfer [13] and the creation of massive quantum superpositions or so-called 'Schrödinger's cat' states [14]–[16]. Here we focus on the latter class of experiments, in particular the one as described in Marshall *et al* [16].

The heart of this experiment is a Michelson interferometer with high finesse optical cavities in each of its arms (figure 1). In one arm the traditional end mirror is replaced with a tiny mirror on a micromechanical cantilever, hereafter referred to as the 'cantilever'. Under the right conditions, the radiation pressure of a single photon in this arm of the experiment will be enough to excite the cantilever into a distinguishable quantum state. A single photon incident on the 50-50 beam splitter will form an optical superposition of being in either of the two arms; the coupling between the photon and the cantilever will then entangle their states, putting the cantilever into a superposition as well. If the photon leaves the interferometer with the cantilever in a distinguishable state, an outside observer could in principle determine which arm the photon took, and so the interference visibility is destroyed. After a full mechanical period of the cantilever, however, it returns to its original position: if the photon leaves the interferometer at this time, the interference visibility should return provided the cantilever was able to remain in a quantum superposition in the intermediate period. Alternatively, if the state of the cantilever collapses during this period due to environmentally induced decoherence, measurement by an

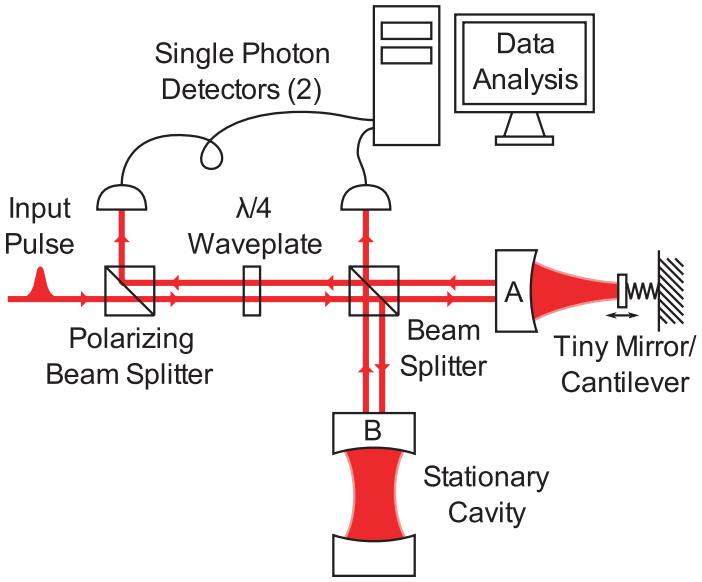

Figure 1. A diagram of the experimental setup. An input pulse is split between the two arms of a Michelson interferometer, labeled A and B, both of which contain high finesse cavities. One end of the cavity in arm A is a tiny end mirror on a micromechanical cantilever, whose motion is affected by the radiation pressure of light in the cavity. Each output port of the interferometer is monitored by a single photon detector, and results are analyzed by a computer to calculate the interference visibility.

outside observer or perhaps an exotic mechanism (e.g. [17]–[19]), the visibility will not return. In this sense the interference revival constitutes evidence that the cantilever was able to exist in a quantum superposition, and a measurement of its magnitude constitutes a measurement of the quantum decoherence in this time interval. In a real experiment, however, one must be careful about drawing conclusions from the visibility dynamics as similar results can be obtained from a fully classical argument.

In this work, we address the issue of classicality by first calculating the quantum dynamics of the system for both a pure state and a thermal density matrix (section 2). We also calculate the Wigner function of the system as a method of determining the transition from the quantum to classical regime (section 3). Finally, we discuss quantum decoherence mechanisms (section 4) and prospects for realization in view of recent experimental results (section 5).

2. Quantum mechanical description

A more detailed analysis of the system begins with the Hamiltonian, given by Law [20]:

$$H = \hbar\omega_a \left[a^\dagger a + b^\dagger b\right] + \hbar\omega_c \left[c^\dagger c - \kappa a^\dagger a \left(c + c^\dagger\right)\right], \tag{1}$$

where ω_a is the frequency of the optical field, $a^\dagger/b^\dagger$ and a/b are the photon creation and annihilation operators for photons the arms A and B of the interferometer, ω_c is the mechanical frequency of the cantilever and $c^\dagger$ and c are the phonon creation and annihilation operators for

its fundamental vibrational mode. The dimensionless optomechanical coupling constant κ is defined as:

$$\kappa = \frac{\omega_a}{L\omega_c}\sqrt{\frac{\hbar}{2m\omega_c}} \tag{2a}$$

$$= \frac{\sqrt{2}Nx_0}{\lambda}, \tag{2b}$$

where m is the mass of the cantilever, L is the length of the optical cavity, N is the number of cavity round trips per mechanical period, λ is the optical wavelength, and $x_0 = \sqrt{\frac{\hbar}{m\omega_c}}$ is the size of the ground state wavepacket for the cantilever. The Hamiltonian treats the mechanical resonator as completely linear, which should be a valid assumption. Nonlinearities have not been observed in experiments conducted on similar systems, which is expected given that the typical vibration amplitudes are many orders of magnitude smaller than the dimensions of the resonator. From this we can derive the unitary evolution operator [14]:

$$\begin{aligned} U(t) = \exp\left[-\mathrm{i}\omega_a t\left(a^\dagger a + b^\dagger b\right) - \mathrm{i}\left(\kappa a^\dagger a\right)^2(\omega_c t - \sin\omega_c t)\right] \\ \times \exp\left[\kappa a^\dagger a\left[\left(1-\mathrm{e}^{-\mathrm{i}\omega_c t}\right)c^\dagger - \left(1-\mathrm{e}^{\mathrm{i}\omega_c t}\right)c\right]\right]\exp\left[-\mathrm{i}\omega_c c^\dagger c t\right]. \end{aligned} \tag{3}$$

2.1. Coherent state

If we consider a cantilever initially in a coherent state with complex amplitude β, the total initial state is given by $|\Psi(0)\rangle = \frac{1}{\sqrt{2}}(|0,1\rangle_{n_a,n_b} + |1,0\rangle_{n_a,n_b}) \otimes |\beta\rangle_c$. Under the action of the unitary operator equation (3) this unentangled state evolves to:

$$\begin{aligned} |\Psi(t)\rangle = \frac{1}{\sqrt{2}}\mathrm{e}^{-\mathrm{i}\omega_a t}\Big(|0,1\rangle \otimes |\beta\mathrm{e}^{-\mathrm{i}\omega_c t}\rangle \\ + \mathrm{e}^{\mathrm{i}\kappa^2(\omega_c t - \sin(\omega_c t)) + \mathrm{i}\kappa\,\mathrm{Im}[\beta(1-\mathrm{e}^{-\mathrm{i}\omega_c t})]}|1,0\rangle \otimes |\kappa(1-\mathrm{e}^{-\mathrm{i}\omega_c t}) + \beta\mathrm{e}^{-\mathrm{i}\omega_c t}\rangle\Big) \end{aligned} \tag{4a}$$

$$= \frac{1}{\sqrt{2}}\mathrm{e}^{-\mathrm{i}\omega_a t}\left(|0,1\rangle \otimes |\Phi_0(t)\rangle + \mathrm{e}^{\mathrm{i}\kappa^2(\omega_c t - \sin(\omega_c t)) - \mathrm{i}\mathrm{Im}[\Phi_0(t)\Phi_1(t)^*]}|1,0\rangle \otimes |\Phi_1(t)\rangle\right). \tag{4b}$$

Because the cantilever is only displaced if the photon is in arm A, the state of the photon and the state of the cantilever become entangled. The cantilever then enters a superposition of two different coherent states, with time dependent amplitude $\Phi_0(t)$ when no photon is present and $\Phi_1(t)$ if there is a photon. After half a mechanical period, the spatial distance between the two cantilever states $|\Phi_0\rangle$ and $|\Phi_1\rangle$ is given by $\Delta x = \sqrt{8}\kappa x_0$, and the two cantilever states have the lowest overlap, $|\langle\Phi_0|\Phi_1\rangle| = \mathrm{e}^{-2\kappa^2}$. After a full mechanical period $|\Phi_0\rangle$ and $|\Phi_1\rangle$ are identical again, and so the photon and cantilever are disentangled. For a proper demonstration of a superposition, we require the overlap between the states to be relatively small during part of the experiment, implying $\kappa \gtrsim 1/\sqrt{2}$. This is equivalent to stipulating that a measurement of the cantilever state alone is sufficient to determine which path a photon took with a reasonable fidelity. As will be discussed in section 5, obtaining this large a value of κ poses the most significant barrier to experimental realization.

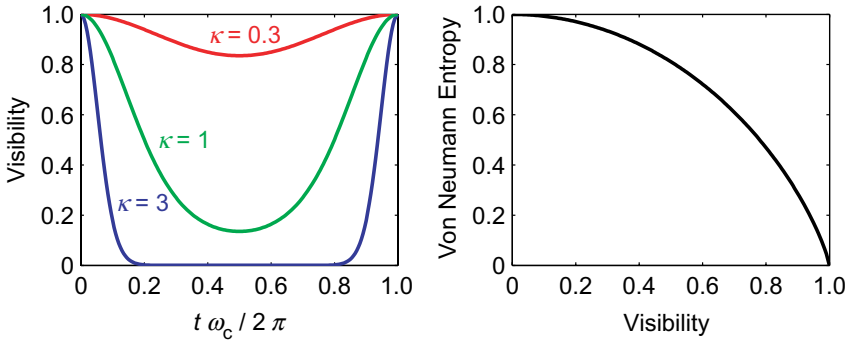

Figure 2. Left panel: the visibility $v(t)$ as a function of time for different values of the optomechanical coupling constant, κ. Right panel: the von Neumann entropy $S(t)$ versus the visibility, $v(t)$.

In practice, the actual quantity measured is the interferometric visibility as seen by the two single photon detectors. This visibility is given by twice the absolute value of the off-diagonal elements of the reduced photon density matrix:

$$v(t) = \mathrm{e}^{-\kappa^2(1-\cos(\omega_c t))}. \tag{5}$$

It exhibits a periodic behavior characterized by a suppression of the interference visibility after half a mechanical period and a revival of perfect visibility after a full period (figure 2) provided there is no decoherence in the state of the cantilever. The visibility can be mapped directly to the entanglement between the photon and the cantilever. For a pure bipartite state, we can express the entanglement as the von Neumann entropy of the photon $S(t)$ in terms of the visibility $v(t)$ (figure 2):

$$S(t) = -\mathrm{Tr}_{\mathrm{ph}}\left(\rho_{\mathrm{ph}} \log_2 \rho_{\mathrm{ph}}\right) \tag{6a}$$

$$= 1 + \frac{v(t)}{2} \log_2\left(\frac{1-v(t)}{1+v(t)}\right) - \frac{1}{2}\log_2\left(1-v(t)^2\right), \tag{6b}$$

where ρ_{ph} is the reduced density matrix for the photon. Since for a pure bipartite system a high von Neumann entropy of one subsystem corresponds to high entanglement between the two subsystems, we conclude that when the initial state is pure, the visibility alone is a good measure for the non-classical behavior of the cantilever. This is true even in the presence of an arbitrary decoherence mechanism, which will destroy the quantum nature of the system and thus produce a corresponding loss of interference visibility.

2.2. The cantilever at finite temperatures

At finite temperatures the exact wavefunction of the cantilever is unknown, so the state is instead described by a density matrix:

$$\rho_c(0) = \frac{\sum_n \mathrm{e}^{-E_n/k_B T}|n\rangle\langle n|}{\sum_n \mathrm{e}^{-E_n/k_B T}} = \frac{1}{\pi\bar{n}}\int \mathrm{d}^2\beta \mathrm{e}^{-|\beta|^2/\bar{n}}|\beta\rangle\langle\beta|, \tag{7}$$

where $\bar{n} = 1/(\mathrm{e}^{\hbar\omega_c/k_B T} - 1)$ is the average thermal occupation number of the cantilever's center of mass mode, $|n\rangle$ are energy eigenstates and $|\beta\rangle$ coherent states of the cantilever. Here, we only

consider the effects of a thermally excited initial state, i.e. for a cantilever with no dissipation ($Q \to \infty$). The effects of dissipation and resulting decoherence are discussed in section 4.

The evolution of equation (7) under the action of equation (3) yields the visibility:

$$v(t) = \mathrm{e}^{-\kappa^2(2\bar{n}+1)(1-\cos(\omega_\mathrm{c} t))}. \tag{8}$$

At finite temperatures the density matrix represents an average over coherent states with different phases which destroys the interference visibility. Although there is also a phase shift from the entanglement as discussed earlier, in principle this shift is known and repeatable, while the same is not true for the thermal state. A good indicator that the visibility no longer captures the quantum behavior is that it becomes independent of $\hbar$ if the initial temperature of the cantilever is high [21]. This can be seen most easily by noting that in the limit $k_\mathrm{b}T \gg \hbar\omega_\mathrm{c}$, the mean phonon number is given by $\bar{n} \approx k_\mathrm{b}T/\hbar\omega_\mathrm{c} - 1/2$. Thus the visibility equation (8) can be rewritten as:

$$v(t) \approx \mathrm{e}^{-(k_\mathrm{b}T/m\omega_\mathrm{c}^2)((2N/\lambda))^2(1-\cos(\omega_\mathrm{c} t))}. \tag{9}$$

This is the classically expected result, which differs primarily from the quantum result in that the visibility is always one at zero temperature because the distinguishability of the cantilever state is irrelevant. At higher temperatures it is difficult to determine when the cantilever was in a superposition state. Because the experiment requires averaging over many runs, the quantum distinguishability is masked by the unknown classical phase shifts.

However, after a full mechanical period the net phase shift from any initial state goes to zero and so full visibility should still return in a narrow window whose width scales like $\bar{n}^{-1/2}$. This leaves open the possibility for measuring quantum collapse mechanisms at higher temperatures if one assumes that the cantilever was in a superposition state. Provided that the optomechanical coupling strength κ is relatively well known (e.g. by independently measuring m, ω_c, L, etc) and the instantaneous quantum state of the cantilever is regarded as some random coherent state (as should be the case for the weakly mechanically damped systems discussed here) it can be easily determined when a superposition should have been created.

Although equation (9) suggests the visibility should always return in the classical case, we note that this can only be true if both the optical *and* mechanical modes are behaving classically. On the other hand, if we regard only the optical field as quantum we should always expect no interference visibility because the classical cantilever would measure which path the photon took. Thus the return of visibility at higher temperatures can be used to strongly imply the existence of a quantum superposition when $\kappa \gtrsim 1/\sqrt{2}$, even though the superposition cannot be directly measured by the visibility loss at $t \sim \pi\omega_\mathrm{c}$.[8]

Nevertheless, an unambiguous demonstration can be provided if the temperature is low enough such that the visibility loss due to quantum distinguishability is still resolvable. At finite cantilever temperatures the interferometric visibility becomes a bad measure for the non-classicality of the mirror. This can be easily seen by the relation between the von Neumann entropy and the visibility, equation (6*b*). It is valid at arbitrary temperatures, but at $T > 0$ the

[8] The presence of a 'loop hole' in such a demonstration could be regarded as analogous to experimental tests of Bell's inequalities, where even though it is generally regarded that quantum mechanics has been adequately demonstrated, an unambiguous proof has remained elusive. In our case, the loop hole is caused by the unknown intermediate state caused by finite temperature. Even though a weakly damped system should produce something that is very nearly a coherent state at any given instance of time, there is no way to directly show the cantilever is in this state.

system is in a mixed state and the entropy is only an upper bound for the entanglement of formation [22]. One thus needs to analyze the non-classicality of the cantilever state by other means. In the next section, we use the integrated negativity of the Wigner function [23] to quantify the non-classicality of the cantilever with respect to temperature.

3. The Wigner function and the classical limit

To study transitions between the quantum and the classical regimes, it is often convenient to refer to quasi-probability distributions, with which quantum mechanics can be formulated in the common classical phase space. One such distribution was proposed in 1932 by Wigner [24] and can be obtained from the density matrix ρ:

$$W(x, p) = \frac{1}{\pi\hbar}\int_{-\infty}^{+\infty} \mathrm{d}y \langle x - y|\rho|x + y\rangle \mathrm{e}^{2\mathrm{i}py/\hbar}. \tag{10}$$

It is well known that in the classical limit $\hbar \to 0$ the Wigner function tends to a classical probability distribution describing a microstate in phase space [25]. This can most easily be seen in the case of a single particle moving in a potential $V(x)$. The time evolution of the Wigner function for this closed system is described by the quantum Liouville equation [24, 26]

$$\left(\frac{\partial}{\partial t} + \frac{p}{m}\frac{\partial}{\partial x} - \frac{\mathrm{d}V(x)}{\mathrm{d}x}\frac{\partial}{\partial p}\right) W(x, p, t) = \sum_{k=1}^{\infty} \hbar^{2k} \frac{(-1)^k}{4^k(2k+1)!} \frac{\mathrm{d}^{2k+1}V(x)}{\mathrm{d}x^{2k+1}} \frac{\partial^{2k+1}}{\partial p^{2k+1}} W(x, p, t). \tag{11}$$

For $\hbar \to 0$, the right-hand side goes to 0, as long as no derivatives diverge. In this limit the Wigner function $W(x, p, t)$ thus evolves according to the classical Liouville equation. However, the quantum nature of $W(x, p, t)$ is also contained in its initial conditions. In fact, in the special case of a harmonic potential, all non-classical behavior is encoded in the initial conditions of the Wigner function only since the right-hand side of equation (11) is always 0. But for $\hbar \to 0$ also the initial conditions become classical and $W(x, p, t)$ can be fully identified with some classical probability density.

If, on the other hand, the Wigner function is negative then no classical interpretation is possible, making it a useful tool to indicate the non-classicality of an arbitrary state. It is thus convenient to quantify the total negativity of the Wigner function [23]:

$$\begin{aligned} N &= \int_{-\infty}^{+\infty} \mathrm{d}x \int_{-\infty}^{+\infty} \mathrm{d}p \,\{|W(x, p)| - W(x, p)\} \\ &= \int \mathrm{d}x \int \mathrm{d}p |W(x, p)| - 1. \end{aligned} \tag{12}$$

For the experiment at hand, we compute the cantilever's Wigner function for dimensionless x and p, with the photon projected into the superposition state $|0, 1\rangle + \mathrm{e}^{\mathrm{i}\theta}|1, 0\rangle$ to avoid destroying the quantum state of the cantilever to which it is entangled. This projection is equivalent to detecting a single photon at one output of the interferometer, where the phase term in the projection accounts for path length differences in the arms. Generally speaking, varying θ shifts the interference peaks but does not modify the Wigner function in a significant way; hereafter we will set it to 0. The resulting Wigner function of the cantilever indeed shows that the system periodically exists in a highly non-classical state (figure 3).

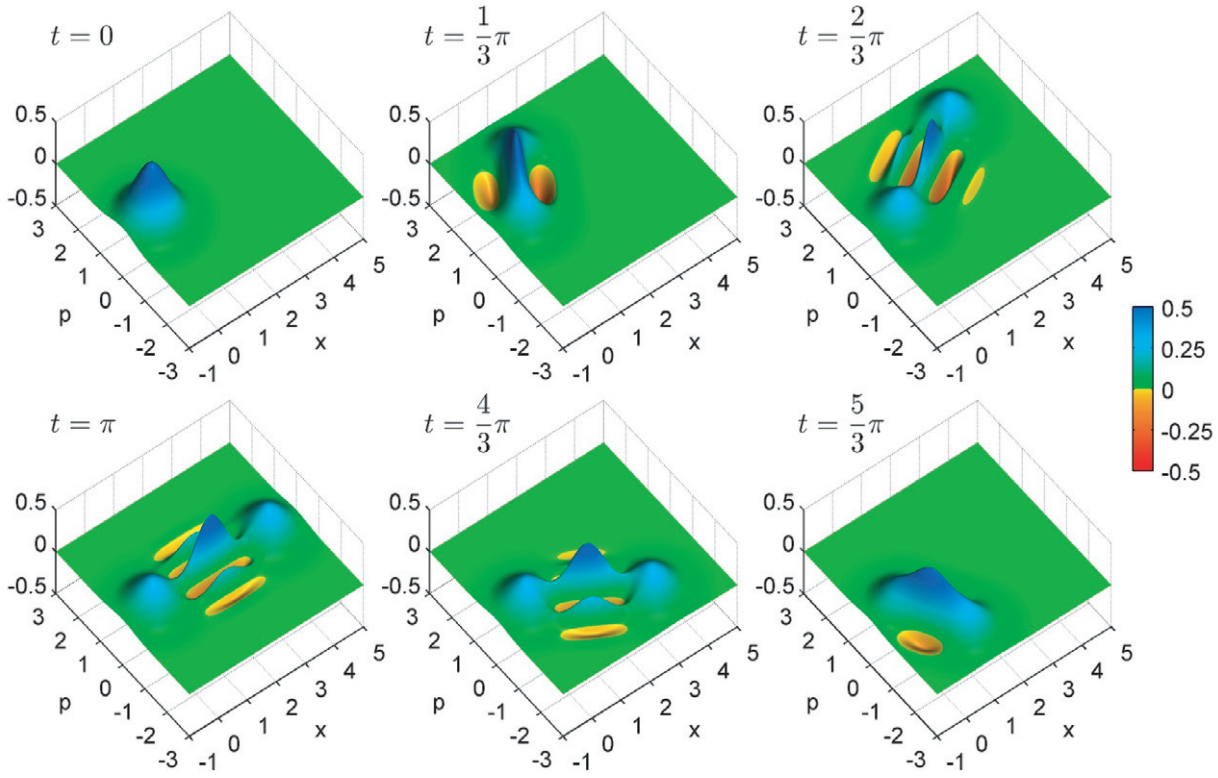

Figure 3. The time evolution of the cantilever's projected Wigner function for $\beta = 0$, $\kappa = 2$ and $\hbar = \omega_c = m = 1$. Regions where the Wigner function is negative, shown in yellow and red, have no classical analogue.

A calculation of the thermally averaged Wigner function shows that the non-classical features are quickly washed out with increasing initial temperature (figure 4). However, as long as part of the Wigner function is negative, the cantilever is clearly in a non-classical superposition state. The negativity of the Wigner function at half a mechanical round trip decreases rapidly with $\bar{n}$ and is also dependent on κ (figure 5). In practice, this implies that $\bar{n}$ must be of order 1 for $\kappa \approx 1$, with somewhat higher values being tolerable for higher κ. This analysis confirms our earlier assertion that direct proof of a superposition requires low mean phonon number.

Finally, we mention that it is also possible to demonstrate the non-classical nature of a mechanical resonator by calculating a measure of entanglement [5]. For example, in a related experiment in which two micromechanical systems are coupled to one another with a light field, the entanglement is lost at higher temperatures [3, 4] (the larger temperature bound obtained is due to a large amplitude coherent state in the optical mode).

4. Decoherence

In addition to 'classical' phase scrambling caused by the initial thermal motion of the cantilever as discussed above, there are other effects which cause 'quantum' decoherence of the cantilever. The signature of this type of decoherence is a reduction of the visibility's revival peak—this is caused by information loss during a single experimental run. This is different from

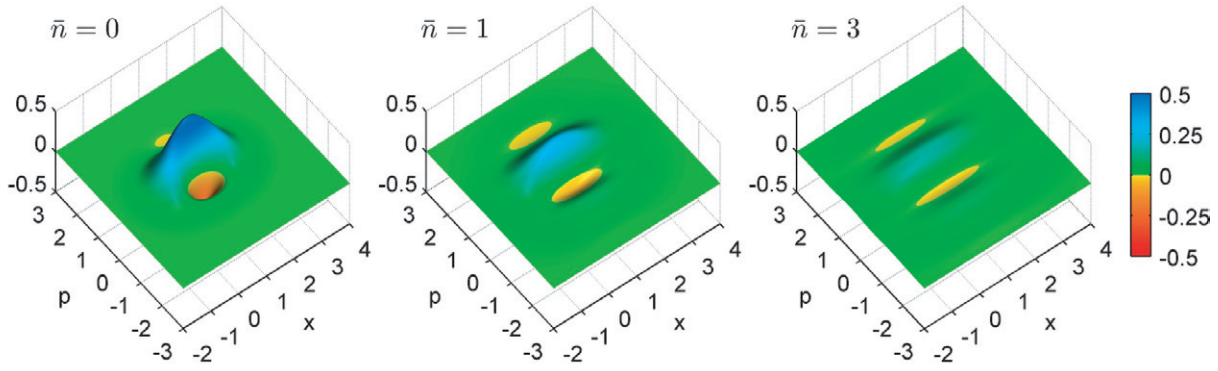

Figure 4. The thermally averaged projected Wigner function of the cantilever at time $t = \pi$ for $\kappa = 1/\sqrt{2}$ and different mean thermal phonon numbers, $\bar{n}$. ($\hbar = \omega_c = m = 1$) The negative regions of the Wigner function, shown in yellow and red, can be seen to quickly wash out with increasing temperature.

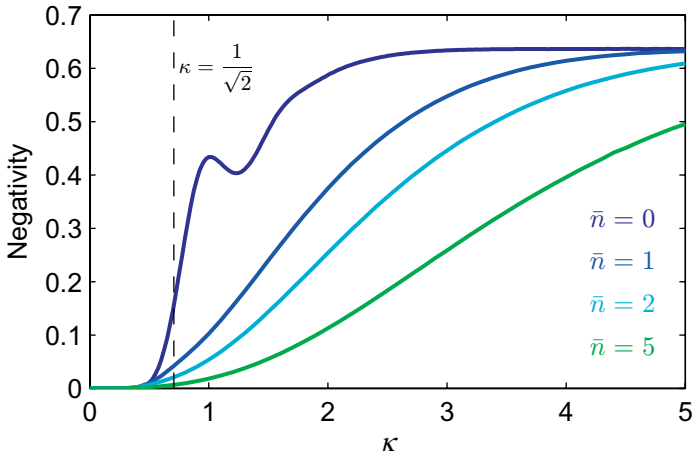

Figure 5. Negativity of the projected cantilever state as a function of coupling constant κ for several different mean phonon numbers, $\bar{n}$. The oscillations present when $\bar{n} = 0$ are due to a phase shift in the interference terms, which are washed out at higher temperatures.

the previously discussed effect which is a narrowing of the visibility revival peaks caused by averaging of states in a thermal mixture, where no information is lost. Thus, to be able to detect a signature of a macroscopic superposition, the timescale on which decoherence occurs should be larger than a single mechanical period.

4.1. Environmentally induced decoherence

Environmentally induced decoherence is due to the coupling of the system to a finite temperature bath, and results in a finite lifetime for the quantum superposition of the cantilever. Decoherence happens when the thermal bath measures the state of the cantilever while the photon is in the cavity, introducing a phase shift that cannot be compensated for even in

principle. To find the timescale for this mechanism we need to solve the open quantum representation of the system. This is generally done by coupling the cantilever to an infinite bath of harmonic oscillators and integrating out the environmental degrees of freedom. In doing so, one obtains a time-local master equation for the density matrix of the system incorporating the influence of the environment.

We start with the Hamiltonian:

$$H = H_{\rm sys} + H_{\rm bath} + H_{\rm int}, \tag{13}$$

where:

$$\begin{aligned} H_{\rm sys} &= \hbar\omega_a \left[a^\dagger a + b^\dagger b\right] + \hbar\omega_c \left[c^\dagger c - \kappa a^\dagger a \left(c + c^\dagger\right)\right], \\ H_{\rm bath} &= \sum_i \hbar\omega_i d_i^\dagger d_i, \\ H_{\rm int} &= (c + c^\dagger) \sum_i \lambda_i (d_i + d_i^\dagger). \end{aligned} \tag{14}$$

Here, $d_i^\dagger$ (d_i) are the creation (annihilation) operators of the bath modes, ω_i is the frequency of each mode and λ_i are coupling constants. Using the Feynman–Vernon influence functional method [27] we can eliminate the bath degrees of freedom. When the thermal energy of the bath sets the highest energy scale we can use the Born–Markov approximation to obtain a master equation for the density matrix of our system [28]:

$$\dot\rho(t) = \frac{1}{{\rm i}\hbar}\left[\tilde H_{\rm sys}, \rho(t)\right] - \frac{{\rm i}\gamma}{\hbar}\left[x, \{p, \rho(t)\}\right] - \frac{D}{\hbar^2}\left[x, [x, \rho(t)]\right], \tag{15}$$

where $\tilde H_{\rm sys}$ is the system Hamiltonian in equation (1), renormalized by the interaction of the cantilever with the bath. $\gamma = \omega_{\rm c}/Q$ is the damping coefficient as determined from the mechanical Q factor and $D = 2m\gamma k_{\rm B} T_{\rm b}$ is the diffusion coefficient where $T_{\rm b}$ is the temperature of the bath. The first term on the right-hand side of (15) is the unitary part of the evolution with a renormalized frequency. The other terms are due to the interaction with the environment only and incorporate the dissipation and diffusion of the cantilever. The equation is valid in the Markovian regime when memory effects in the bath can be neglected; this is satisfied when the coupling to the bath is weak ($Q \gg 1$) and the thermal energy is much higher than the phonon energy ($k_{\rm B} T_{\rm b} \gg \hbar\omega_{\rm c}$). Both conditions are easily satisfied for realistic devices.

Following Zurek [29], we note that in the macroscopic regime (to highest order in $\hbar^{-1}$), the master equation is dominated by the diffusion term proportional to $D/\hbar^2$. Evaluating it in the position basis, one finds the timescale:

$$\tau_{\rm dec} = \frac{\hbar^2}{D(\Delta x)^2} = \frac{\hbar Q}{16 k_{\rm B} T_{\rm b} \kappa^2}, \tag{16}$$

where $\Delta x = \sqrt{8}\kappa x_0$, as before. A calculation of the Wigner function which includes decoherence of the off-diagonal elements with the above dependence shows how the non-classicality of the state is dissipated with time (figure 6).

An exact open quantum system analysis of the experimental setup based on equation (15) has been performed by Bassi *et al* [30] and Bernád *et al* [21]. The former authors neglect the term proportional to p in equation (15) and solve the resulting equation for the off-diagonal matrix elements of the reduced photon density matrix. The latter authors use the full equation. The results for the decoherence of the revival peaks in these papers are remarkably close to the

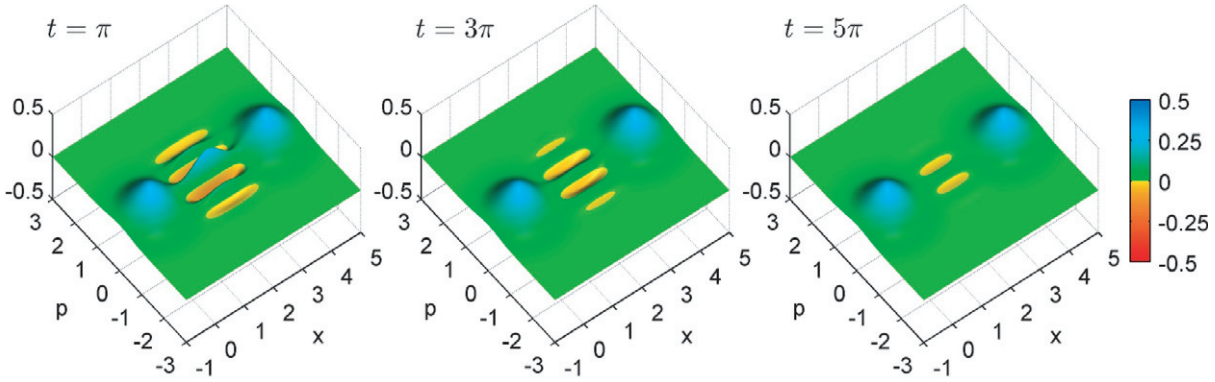

Figure 6. Wigner function of the system in the presence of environmentally induced decoherence for $T_b = T_{EID}/64$, $\kappa = 2$ and $\hbar = \omega_c = m = 1$.

above estimate, both predicting a longer coherence time by only a factor of 8/3. The order of magnitude is thus well captured by (16).

For an optomechanical system the important parameter is the mechanical quality factor, Q. It is convenient to define a characteristic environmentally induced decoherence temperature:

$$T_{EID} = \frac{\hbar\omega_c Q}{k_B}. \tag{17}$$

With this definition, the decoherence time (16) can be written as $\tau_{dec}^{-1} = 16\kappa^2\omega_c(\frac{T_b}{T_{EID}})$. Above this temperature the interference revival peak will be drastically reduced in magnitude. We note that the environmentally induced decoherence rate is dependent only on the bath temperature, T_b, not the effective temperature of the cantilever mode, T, which can be made different from the bath temperature by optical cooling (see section 5.2). Since a high-Q resonator is only weakly coupled to the bath, it is sufficient to treat these two temperatures as independent.

4.2. Gravitationally induced quantum collapse

To explain the apparent classicality of the macroscopic world, it has been suggested that there may be a quantum state collapse mechanism for large objects, possibly induced by mass. Several proposals have been made which lead to such a collapse, among them reformulations of quantum mechanics [31, 32] and the use of the intrinsic incompatibility between general relativity and quantum mechanics [17]–[19]. Unlike environmentally induced decoherence, which is largely a nuisance in the realization of a massive superposition experiment, measurement of a mass-induced collapse would be evidence of new physics and is hence of considerable interest.

Here we review the gravitational collapse model given by Penrose [18]. Penrose argues that a superposition of a massive object will result in a co-existence of two different space–time geometries which cannot be matched in a coordinate independent way. Any difference in the causal structure will then generate different time translation operators $\partial/\partial t$ in the respective space–times. Only an asymptotic identification would be possible, but if a local notion is required the failure to identify a single time structure for two superposed space–times will be a fundamental obstacle to unitary quantum evolution. Any time translation operator $\partial/\partial t$ in such

a superposition of space-times will have an intrinsic error and hence a unitary evolution cannot take place indefinitely. This will eventually result in a collapse of the superposed state.

To give an order of magnitude estimate for the identification of the two superposed space-times, Penrose uses the Newtonian limit of gravity including the principle of general covariance. The error is quantified by the difference of free falls (geodesics) throughout both space–times, which turns out to correspond to the gravitational self energy ΔE of the superposed system, defined the following way:

$$E_{i,j} = -G \int\int \mathrm{d}\vec{r}_1 \mathrm{d}\vec{r}_2 \frac{\rho_i(\vec{r}_1)\rho_j(\vec{r}_2)}{|\vec{r}_1 - \vec{r}_2|}, \tag{18a}$$

$$\Delta E = 2E_{1,2} - E_{1,1} - E_{2,2}, \tag{18b}$$

where ρ_1 and ρ_2 are the mass distributions for the two states in question. A similar result was obtained by Diosi [19]. This energy yields a timescale for the decay of a superposition given by $\tau_G \approx \hbar/\Delta E$.

When attempting to apply this to the proposed superposition experiment, it is unclear precisely what form the mass distributions should take (see also [33]). For simplicity we will consider the mass to be evenly distributed over a number of spheres, corresponding to atomic nuclei, each with mass m_1, radius a, and the superposition states to be separated by a distance Δx. The total mass is given by m, as before. If the atomic spacing is much larger than the effective mass radius, the energy due to the interaction between different atomic sites is negligible and the gravitational self-energy is given by:

$$\Delta E = 2Gmm_1\left(\frac{6}{5a} - \frac{1}{\Delta x}\right), \quad (\text{given: } \Delta x \geqslant 2a). \tag{19}$$

If we set the sphere radius to be the approximate size of a nucleus ($a = 10^{-15}$ m) and use the parameters of an ideal optomechanical device ($m = 10^{-12}$ kg, $\omega_c = 2\pi \times 1$ kHz, $\kappa = 1/\sqrt{2}$ and $m_1 = 4.7 \times 10^{-26}$ kg, the silicon nuclear mass), this results in a timescale of the order of milliseconds. Alternatively, one could argue that the effective diameter of the spheres should be the ground-state wavepacket size ($a = x_0/2$). With the maximum separation of the states ($\Delta x = \sqrt{8}\kappa x_0$), the resulting energy is:

$$\Delta E = \frac{Gmm_1}{x_0}\left(\frac{24}{5} - \frac{1}{\sqrt{2}\kappa}\right). \tag{20}$$

Using the ideal device parameters results in a timescale of the order of 1 s.

In order to practically measure such a collapse mechanism, we require the timescale to be not much larger than a mechanical period so that a significant visibility reduction is present in the first revival peak. This means it may be possible to measure a mass-induced collapse effect with the proposed experiment, although we note that the collapse timescale given above is intended only to be a rough estimate. To contrast with previous large superposition experiments, the collapse timescale for interferometry of large molecules like C_{60} [34] is calculated to be 10^{10} s (using the nuclear radius, $a = 10^{-15}$ m, and assuming comparatively larger separation). Other demonstrated experiments have similar or larger timescales, meaning a collapse mechanism of this type would have certainly been undetectable in all experiments to date.

5. Prospects for experimental realization

5.1. Optomechanical devices

In practice, the experimental realization of a macroscopic quantum superposition is severely technically demanding. Perhaps the most challenging aspect is achieving sufficient optical quality, which is required to put the cantilever into a distinguishable state via interaction with a single photon, i.e. $\kappa \gtrsim 1/\sqrt{2}$. Although κ can be increased by shortening the optical cavity, this will also reduce the ring-down time, making it extremely unlikely to observe a photon in the revival period. A reasonable compromise is reached by requiring the optical finesse, F, to be equal to the required number of round trips per period as given by (2*b*). In this case, the fraction of photons still in the optical cavity after a mechanical period is $e^{-2\pi}$ (0.2%), a small number but enough to measure the visibility on the timescale of hours. This resulting requirement for the finesse has a rather intuitive form:

$$F \gtrsim \frac{\lambda}{2x_0}. \tag{21}$$

In order to prevent diffraction from limiting the finesse, the mirror on the cantilever needs a diameter of order 10 μm or larger [35]. If the mirror is a dielectric Bragg reflector, the conventional choice for achieving very high optical quality, the required finesse is of order 10^6–10^7 given the minimum resulting mass and assuming it is placed on a cantilever with frequency $\sim$1 kHz. Finesses of over 10^6 have been realized in several experiments with larger, cm size, dielectric mirrors (for example [36]), so the primary challenge in using these mirrors is finding a way to micro-fabricate them without degrading their properties. State of the art is currently $F = 10^4$–10^5, although rapid progress has been made in recent years due to a growing interest in optomechanical systems in general. See figure 7 for a comparison of different devices. An interesting alternative to the tiny mirror on the cantilever approach is the so-called 'membrane in the middle'. In this case the optomechanical element is a dielectric membrane placed between two high quality mirrors; the cavity detuning induced by motion of the membrane produces a result functionally equivalent to moving an end mirror on a mechanical resonator. Commercially available silicon nitride membranes have recently been demonstrated in cavities with finesses of over 10^4 and with remarkably high mechanical quality factors, $Q > 10^7$ [37]. In theory, this type of system would require a lower finesse to achieve a superposition, as the thickness of the optical element can be an order of magnitude less than a dielectric mirror. To take advantage of this, however, would require the membranes be micro-fabricated into cantilever or bridge-resonator structures to reduce their total mass, something that has not yet been attempted.

The other important parameter for an optomechanical system is the mechanical quality factor, Q, governing the characteristic environmentally induced decoherence temperature T_{EID}, as defined in (17). Optomechanical devices have already been demonstrated for which T_{EID} is experimentally accessible with common cryogenic techniques (figure 7), although operating the devices in the sub-Kelvin regime is likely to be difficult. Resonators used in magnetic force resonance microscopy experiments, which have similar mechanical properties, have been cooled to temperatures of around 100 mK, limited by heating due to optical absorption in the readout [39]. Although the magnitude of this effect should be smaller for high finesse optomechanical systems due to lower absorption and incident light levels, at temperatures of order 1 mK absorption of even single photons should produce non-negligible heating [44].

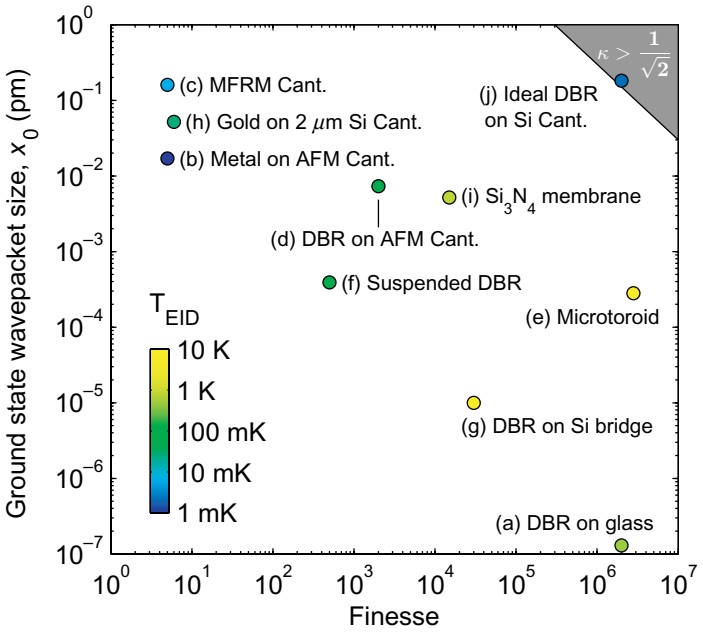

Figure 7. A comparison of optomechanical devices, showing the finesse and size of the ground-state wavepacket, $x_0 = \sqrt{\hbar/m\omega_c}$. All points apart from (j) are based on experimental results. The shaded area in the upper right corresponds to $\kappa = 1/\sqrt{2}$ for visible light ($\lambda = 600\,\mathrm{nm}$). The color of each point corresponds to the characteristic environmentally induced decoherence temperature, $T_{\mathrm{EID}} = \hbar\omega_c Q/k_b$. Many of the devices are the subject of ongoing research, and so the listed parameters should be regarded as approximate. (a) A dielectric Bragg reflector (DBR) with $F = 2 \times 10^6$ deposited on a cm size mirror. (b) Metal deposited on a conventional atomic force microscopy (AFM) cantilever (for example, [38]). (c) A thin silicon cantilever used in magnetic force resonance microscopy (MFRM) [39]. (d) A focused ion beam milled DBR mirror glued to a commercial AFM cantilever [35]. (e) Microtoroidal resonator [40]. (κ is not given by (2*b*) because of a different geometry.) (f) Resonator made of a suspended DBR bridge [41]. (g) DBR deposited on a silicon bridge resonator [42]. (h) A 2 μm silicon resonator with gold deposited on it [43]. (i) Commercial Si_3N_4 membrane in a high finesse optical cavity [37]. (j) Theoretical device with a tiny, high finesse DBR mirror attached to a cantilever similar to those used in MFRM experiments ($m = 10^{-12}\,\mathrm{kg}$, $\omega_c = 2\pi \times 500\,\mathrm{Hz}$, $F = 2 \times 10^6$).

5.2. Optical cooling

As stated above, unambiguous observation of a macroscopic quantum superposition is possible only when the cantilever's fundamental mode is in a low phonon quantum number state. Given that this requires temperatures of less than 1 μK for kHz resonators, the only way to practically obtain this is optical feedback cooling. There are two primary forms of optical feedback cooling, referred to as 'active' and 'passive'. Active feedback cooling uses the optical cavity to read out the position of the cantilever, and then an electronic feedback loop creates a force on

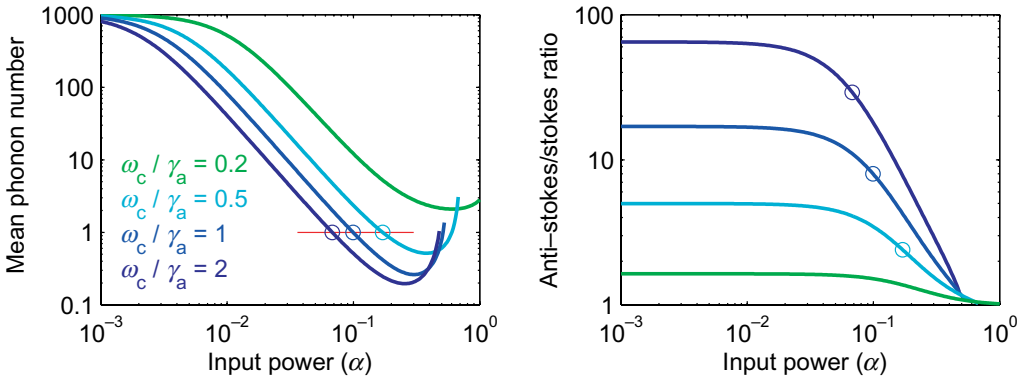

Figure 8. Left panel: mean phonon number, $\bar{n}$ as a function of power for passive optical feedback cooling. Right panel: anti-Stokes/Stokes ratio. The theoretical model is derived from Marquardt *et al* [9]. The input optical field strength is given in terms of a dimensionless power, $\alpha = \sqrt{2\bar{n}_a}\kappa$ where $\bar{n}_a$ is the mean number of photons in the optical cavity. γ_a is the power decay constant for the optical cavity. Pump photons are detuned from the cavity resonance by $\Delta = -\omega_c$. When $\bar{n} = 1$, the anti-Stokes/Stokes ratio decreases to half its low field ($\alpha \to 0$) limit, shown with circles in (b). The ratio, which can be measured in the light leaving the cavity, provides a direct method to determine the effective temperature of the cantilever.

the cantilever (using, e.g. a second intensity modulated laser) to dampen the motion of its fundamental mode. Because the effective damping force is not subjected to thermal fluctuations, this is equivalent to coupling the system to a zero temperature thermal bath, and so the effective temperature of the fundamental mode can be dramatically reduced. Passive feedback cooling uses the finite ring-down time of the optical cavity to intrinsically produce a similar damping force without the use of an external feedback loop. Note that neither type of cooling significantly reduces the temperature of the environmental bath, so the environmentally induced decoherence timescale is virtually unaffected by optical cooling. Both active [44]–[46] and passive [12], [40]–[43], [47]–[50] feedback cooling have been experimentally demonstrated by many groups, in some cases achieving cooling factors of well over 10^3.

If one operates below the environmentally induced decoherence temperature given above, it is theoretically possible to cool the fundamental mode of the cantilever near the ground state using either active [7] or passive optical feedback cooling [8]–[10], although this has yet to be demonstrated experimentally. Although heating due to optical absorption and linewidth of the drive laser are serious concerns [51], these do not present fundamental obstacles. In the limit that the ring-down time is comparable to the mechanical period, as indeed it must be for observing a macroscopic superposition, passive cooling should be more effective. The equilibrium phonon occupation number of the cantilever as a function of pumping power is shown in figure 8; the situation where $N = F$, as discussed above, corresponds to $\omega_c/\gamma_a = 1$. Conveniently, passive cooling also provides a method to directly measure the phonon number of the cantilever by measuring the ratio of anti-Stokes to Stokes shifted photons in the outgoing cavity field (see also figure 8) [8, 9]. In the limit of low pumping power and minimal cooling, this ratio remains constant, but begins to rapidly decrease when the ground state is approached. When the ratio is

less than half the low power value, the mean phonon number, $\bar{n}$, is less than one, providing a clear indication of ground state cooling. Because this type of cooling can be easily integrated with the proposed macroscopic superposition experiment, it presents an ideal method for putting the system in a known low phonon number state.

6. Conclusion

A detailed analysis of the effects of finite temperature on the proposed massive superposition experiments show that a fully unambiguous demonstration requires low fundamental mode temperatures, $\bar{n} \lesssim 1$. Despite this, observation of a revival of the interference visibility can be used to strongly imply the existence of a superposition at higher temperatures, as proposed in [16]. Additionally, the magnitude of the visibility revival provides an opportunity to test environmentally induced decoherence models and possibly measure proposed mass-induced collapse mechanisms. Although such an experiment is difficult to realize, comparison to several related experiments suggests it should be technologically feasible. This is greatly aided by growing interest in developing high quality micro-optomechanical devices for a range of applications. Additionally, recently developed optical feedback cooling techniques can be used to obtain fundamental mode temperatures far lower than are conventionally accessible, possibly even cooling to the ground state.

Acknowledgments

We thank C Simon and L Diosi for useful discussions. I P thanks J Bosse for support. This work was supported in part by the National Science Foundation (grants PHY-0504825 and PHY05-51164), Marie-Curie EXT-CT-2006-042580 and the Stichting voor Fundamenteel Onderzoek der Materie (FOM).

References

[1] Mancini S, Vitali D, Giovannetti V and Tombesi P 2003 Stationary entanglement between macroscopic mechanical oscillators *Eur. Phys. J.* D **22** 417–22

[2] Pinard M, Dantan A, Vitali D, Arcizet O, Briant T and Heidmann A 2005 Entangling movable mirrors in a double cavity system *Europhys. Lett.* **72** 747

[3] Vitali D, Mancini S and Tombesi P 2007 Stationary entanglement between two movable mirrors in a classically driven Fabry–Perot cavity *J. Phys. A: Math. Theor.* **40** 8055–68

[4] Vitali D, Gigan S, Ferreira A, Böhm H R, Tombesi P, Guerreiro A, Vedral V, Zeilinger A and Aspelmeyer M 2007 Optomechanical entanglement between a movable mirror and a cavity field *Phys. Rev. Lett.* **98** 030405

[5] Paternostro M, Vitali D, Gigan S, Kim M S, Brukner C, Eisert J and Aspelmeyer M 2007 Creating and probing multipartite macroscopic entanglement with light *Phys. Rev. Lett.* **99** 250401

[6] Giovannetti V, Mancini S and Tombesi P 2001 Radiation pressure induced Einstein–Podolsky–Rosen paradox *Europhys. Lett.* **54** 559–65

[7] Courty J-M, Heidmann A and Pinard M 2001 Quantum limits of cold damping with optomechanical coupling *Eur. Phys. J.* D **17** 399–408

[8] Wilson-Rae I, Nooshi N, Zwerger W and Kippenberg T J 2007 Theory of ground state cooling of a mechanical oscillator using dynamical backaction *Phys. Rev. Lett.* **99** 093901

[9] Marquardt F, Chen J P, Clerk A A and Girvin S M 2007 Quantum theory of cavity-assisted sideband cooling of mechanical motion *Phys. Rev. Lett.* **99** 093902
[10] Bhattacharya M and Meystre P 2007 Trapping and cooling a mirror to its quantum mechanical ground state *Phys. Rev. Lett.* **99** 073601
[11] Bhattacharya M, Uys H and Meystre P 2008 Optomechanical trapping and cooling of partially reflective mirrors *Phys. Rev.* A **77** 033819
[12] Thompson J D, Zwickl B M, Jayich A M, Marquardt F, Girvin S M and Harris J G E 2008 Strong dispersive coupling of a high-finesse cavity to a micromechanical membrane *Nature* **452** 72–5
[13] Zhang J, Peng K and Braunstein S L 2003 Quantum-state transfer from light to macroscopic oscillators *Phys. Rev.* A **68** 013808
[14] Bose S, Jacobs K and Knight P L 1997 Preparation of nonclassical states in cavities with a moving mirror *Phys. Rev.* A **56** 4175–86
[15] Bose S, Jacobs K and Knight P L 1999 Scheme to probe the decoherence of a macroscopic object *Phys. Rev.* A **59** 3204–10
[16] Marshall W, Simon C, Penrose R and Bouwmeester D 2003 Towards quantum superpositions of a mirror 2003 *Phys. Rev. Lett.* **91** 130401
[17] Károlyházy F 1966 Gravitation and quantum mechanics of macroscopic objects *Nuovo Cimento* A **42** 390–402
[18] Penrose R 1996 On gravity's role in quantum state reduction *Gen. Relativ. Gravit.* **28** 581–600
[19] Diósi L 1989 Models for universal reduction of macroscopic quantum fluctuations *Phys. Rev.* A **40** 1165–74
[20] Law C K 1995 Interaction between a moving mirror and radiation pressure: a Hamiltonian formulation *Phys. Rev.* A **51** 2537–41
[21] Zsolt Bernád J, Diósi L and Geszti T 2006 Quest for quantum superpositions of a mirror: high and moderately low temperatures *Phys. Rev. Lett.* **97** 250404
[22] Nielsen M A, Chuang I L and James D F V 2001 Quantum computation and quantum information *Phys. Today* **54** 60–2
[23] Kenfack A and Zyczkowski K 2004 Negativity of the Wigner function as an indicator of non-classicality *J. Opt. B: Quantum Semiclass. Opt.* **6** 396–404
[24] Wigner E 1932 On the quantum correction For thermodynamic equilibrium *Phys. Rev.* **40** 749–59
[25] Hillery M, O'Connell R F, Scully M O and Wigner E P 1984 Distribution functions in physics: fundamentals *Phys. Rep.* **106** 121–67
[26] Schleich W P 2001 *Quantum Optics in Phase Space* (New York: Wiley-VCH)
[27] Feynman R P and Vernon F L Jr 1963 The theory of a general quantum system interacting with a linear dissipative system *Ann. Phys.* **24** 118–73
[28] Caldeira A O and Leggett A J 1983 Path integral approach to quantum Brownian motion *Physica* A **121** 587–616
[29] Zurek W H 2003 Decoherence, einselection, and the quantum origins of the classical *Rev. Mod. Phys.* **75** 715–75
[30] Bassi A, Ippoliti E and Adler S L 2005 Towards quantum superpositions of a mirror: an exact open systems analysis *Phys. Rev. Lett.* **94** 030401
[31] Ghirardi G C, Rimini A and Weber T 1986 Unified dynamics for microscopic and macroscopic systems *Phys. Rev.* D **34** 470–91
[32] Weinberg S 1989 Testing quantum mechanics *Ann. Phys.* **194** 336–86
[33] Diósi L 2007 Notes on certain Newton gravity mechanisms of wavefunction localization and decoherence *J. Phys. A: Math. Theor.* **40** 2989–95
[34] Arndt M, Nairz O, Vos-Andreae J, Keller C, van der Zouw G and Zeilinger A 1999 Wave-particle duality of C_{60} molecules *Nature* **401** 680–2
[35] Kleckner D, Marshall W, de Dood M J A, Dinyari K N, Pors B-J, Irvine W T M and Bouwmeester D 2006 High finesse opto-mechanical cavity with a movable thirty-micron-size mirror *Phys. Rev. Lett.* **96** 173901

[36] Rempe G, Thompson R J, Kimble H J and Lalezari R 1992 Measurement of ultralow losses in an optical interferometer *Opt. Lett.* **17** 363–5
[37] Zwickl B M, Shanks W E, Jayich A M, Yang C, Jayich A C B, Thompson J D and Harris J G E 2008 High quality mechanical and optical properties of commercial silicon nitride membranes *Appl. Phys. Lett.* **92** 103125
[38] Mamin H J and Rugar D 2001 Sub-attonewton force detection at millikelvin temperatures *Appl. Phys. Lett.* **79** 3358–60
[39] Kleckner D and Bouwmeester D 2006 Sub-kelvin optical cooling of a micromechanical resonator *Nature* **444** 75–8
[40] Metzger C H and Karrai K 2004 Cavity cooling of a microlever *Nature* **432** 1002–5
[41] Schliesser A, Rivière R, Anetsberger G, Arcizet O and Kippenberg T J 2008 Resolved sideband cooling of a micromechanical oscillator *Nat. Phys.* **4** 415–9
[42] Gigan S, Böhm H R, Paternostro M, Blaser F, Langer G, Hertzberg J B, Schwab K C, Bäuerle D, Aspelmeyer M and Zeilinger A 2006 Self-cooling of a micromirror by radiation pressure *Nature* **444** 67–70
[43] Arcizet O, Cohadon P-F, Briant T, Pinard M and Heidmann A 2006 Radiation-pressure cooling and optomechanical instability of a micromirror *Nature* **444** 71–4
[44] Favero I, Metzger C, Camerer S, König D, Lorenz H, Kotthaus J P and Karrai K 2007 Optical cooling of a micromirror of wavelength size *Appl. Phys. Lett.* **90** 4101
[45] Cohadon P F, Heidmann A and Pinard M 1999 Cooling of a mirror by radiation pressure *Phys. Rev. Lett.* **83** 3174–7
[46] Poggio M, Degen C L, Mamin H J and Rugar D 2007 Feedback cooling of a Cantilever's fundamental mode below 5 mK *Phys. Rev. Lett.* **99** 017201
[47] Schliesser A, Del'Haye P, Nooshi N, Vahala K J and Kippenberg T J 2006 Radiation pressure cooling of a micromechanical oscillator using dynamical backaction *Phys. Rev. Lett.* **97** 243905
[48] Corbitt T, Chen Y, Innerhofer E, Müller-Ebhardt H, Ottaway D, Rehbein H, Sigg D, Whitcomb S, Wipf C and Mavalvala N 2007 An all-optical trap for a gram-scale mirror *Phys. Rev. Lett.* **98** 150802
[49] Gröblacher S, Gigan S, Böhm H R, Zeilinger A and Aspelmeyer M 2008 Radiation-pressure self-cooling of a micromirror in a cryogenic environment *Europhys. Lett.* **81** 54003
[50] Corbitt T, Wipf C, Bodiya T, Ottaway D, Sigg D, Smith N, Whitcomb S and Mavalvala N 2007 Optical dilution and feedback cooling of a gram-scale oscillator to 6.9 mK *Phys. Rev. Lett.* **99** 160801
[51] Diosi L 2008 Laser linewidth hazard in optomechanical cooling *Phys. Rev.* A **78** 021801